Available online at www.sciencedirect.com
SCIENCE DIRECT®
ELSEVIER
Journal of Sound and Vibration 289 (2006) 413–420
JOURNAL OF SOUND AND VIBRATION
www.elsevier.com/locate/jsvi

Short Communication

Flapwise bending vibration analysis of a rotating tapered cantilever Bernoulli–Euler beam by differential transform method

Ö. Özdemir, M.O. Kaya*

Faculty of Aeronautics and Astronautics, İstanbul Technical University, 34469 Maslak, İstanbul, Turkey

Received 6 July 2004; received in revised form 11 January 2005; accepted 31 January 2005
Available online 16 June 2005

Abstract

This paper studies the vibration characteristics of a rotating tapered cantilever Bernoulli–Euler beam with linearly varying rectangular cross-section of area proportional to x^n, where n equals to 1 or 2 covers the most practical cases. In this work, the differential transform method (DTM) is used to find the nondimensional natural frequencies of the tapered beam. Numerical results are tabulated for different taper ratios, nondimensional angular velocities and nondimensional hub radius. The effects of the taper ratio, nondimensional angular velocity and nondimensional hub radius are discussed. The accuracy is assured from the convergence of the natural frequencies and from the comparisons made with the studies in the open literature. It is shown that the natural frequencies of a rotating tapered cantilever Bernoulli–Euler beam can be obtained with high accuracy by using DTM.

1. Introduction

The differential transform method (DTM) is based on the Taylor series expansion and appears to have been first introduced by Zhou in 1986 [1]. It has been applied to vibration analysis of a tapered bar recently [2]. In this contest Chung and Yoo developed a new dynamic modeling method using stretch deformation [3]. They showed that, two of the linear differential equations

*Corresponding author. Tel.: +90 212 2853110; fax: +90 212 2852926.
E-mail address: kayam@itu.edu.tr (M.O. Kaya).

0022-460X/$ - see front matter © 2005 Published by Elsevier Ltd.
doi:10.1016/j.jsv.2005.01.055

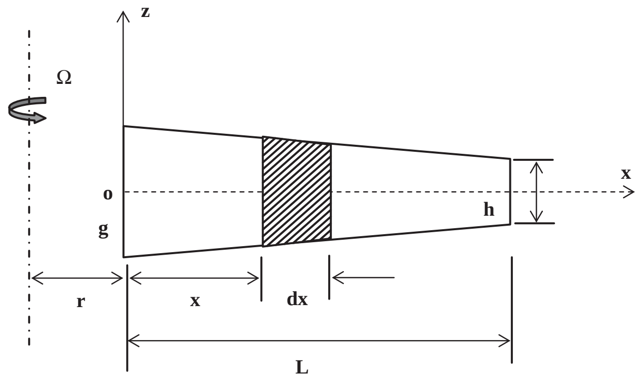

Fig. 1. Configuration of a rotating tapered cantilever Bernoulli–Euler beam.

are coupled through the stretch (i.e. in the radial direction) and the chordwise (i.e. in the plane of rotation) deformations. On the other hand, the differential equation related to the flapwise (i.e. in the direction perpendicular to the plane of rotation) deformation was considered to be uncoupled.

In this work, flapwise bending vibration of a rotating tapered cantilever Bernoulli–Euler beam is studied by using the DTM. In Fig. 1, a cantilever tapered beam of length L, which tapers to a height h and which is fixed at point o to a rigid hub with radius r, is shown. The beam is assumed to be rotating at a constant angular velocity Ω. In the right-handed Cartesian coordinate system shown, the origin is taken to be at the left-hand end of the beam. The X-axis coincides with the neutral axis of the beam in the undeflected position, the Z-axis is parallel to the axis of rotation (but not coincidental) and the Y-axis lies in the plane of rotation. The principal axes of the beam cross-sections are, therefore, parallel to Y and Z directions, respectively. The system is able to flex in the Z direction (flapping motion) and in the Y direction (lead-lag motion). These two motions can be coupled only through Coriolis forces, but for the system shown in the present analysis, this coupling is ignored.

2. Equation of motion

The assumptions for the tapered beam are as follows

$$A(x) = A_g\left(1 - \frac{cx}{L}\right)^n, \tag{1}$$

$$I_{yy}(x) = I_{yyg}\left(1 - \frac{cx}{L}\right)^{n+2}, \tag{2}$$

$$I_{zz}(x) = I_{zzg}\left(1 - \frac{cx}{L}\right)^{n+2}, \tag{3}$$

where A, I_{yy}, I_{zz} are the cross-sectional area and second moment of areas about the Y and Z axes, respectively. The subscript g denotes a value at g in Fig. 1 corresponding to the left-hand end of the tapered beam and c is a constant called the taper ratio which must be such that $c<1$ because otherwise the beam tapers to zero between its ends. Values of $n=1$ or 2 cover the most practical cases because $n=1$ gives linear variation of the area of the cross-section and cubic variation of the second moment of area along the length, whereas $n=2$ are the second and fourth orders. Thus, a large number of solids or thin-walled cross-sections can be represented by using the values of n as 1 or 2. Young's modulus E, shear modulus G and density of the material ρ, are assumed to be constant so that the mass per unit length ρA, the bending rigidities EI_{yy} and EI_{zz} and the shear rigidity kAG vary according to Eqs. (1)–(3) [4].

The centrifugal tension force $T(x)$ at a distance x from the origin is given by

$$T(x) = \int_x^L \rho A \Omega^2 (r + x)\,\mathrm{d}x. \tag{4}$$

According to the Bernoulli–Euler theory, the governing differential equation for the flapwise bending motion is given by

$$\rho A \frac{\partial^2 w}{\partial t^2} + \frac{\partial^2}{\partial x^2}\left(EI \frac{\partial^2 w}{\partial x^2}\right) - \frac{\partial}{\partial x}\left(T \frac{\partial w}{\partial x}\right) = p_w, \tag{5}$$

where w is the deflection and p_w is the applied force per unit length, both in the flapwise direction. For a cantilever beam, four boundary conditions are given by

$$w = \frac{\partial w}{\partial x} = 0 \quad \text{at } x = 0, \tag{6}$$

$$\frac{\partial^2 w}{\partial x^2} = \frac{\partial^3 w}{\partial x^3} = 0 \quad \text{at } x = L. \tag{7}$$

3. Nondimesionalisation of principal parameters

The dimensionless parameters for the element location, the hub radius and the angular velocity respectively are as follows [5]:

$$\xi = \frac{x}{L}, \quad \delta = \frac{r}{L}, \quad \gamma^2 = \frac{\rho A_g \Omega^2 L^4}{EI_g}. \tag{8}$$

Substituting the dimensionless parameters and the tapered beam assumptions into Eq. (4) will lead to the nondimensional centrifugal tension force expression

$$T = M\left[(1 - c\xi)^{n+1}(1 + 2c\delta + cn\delta + c\xi + nc\xi) - (1 - c)^{n+1}(1 + 2c\delta + cn\delta + c + nc)\right], \tag{9}$$

where

$$M = \frac{\rho A_g \Omega^2 L^2}{c^2(n+2)(n+1)}.$$

By substituting this nondimensional centrifugal tension force expression into the flapwise bending equation and accepting $n=1$, Eq. (5) becomes

$$\begin{aligned}&\frac{1}{\gamma^2}\frac{\mathrm{d}}{\mathrm{d}\xi^2}\left[(1-c\xi)^3\frac{\mathrm{d}^2w}{\mathrm{d}\xi^2}\right]-w\lambda^2(1-c\xi)\\&-\frac{1}{6c^2}\frac{\mathrm{d}}{\mathrm{d}\xi}\left\{\left[(1-c\xi)^2(1+3\delta c+2c\xi)-(1-c)^2(1+3\delta c+2c)\right]\frac{\mathrm{d}w}{\mathrm{d}\xi}\right\}=0.\end{aligned} \tag{10}$$

By using the dimensionless parameters, the boundary conditions stated in Eqs. (6) and (7) can be expressed as

$$w=\frac{\mathrm{d}w}{\mathrm{d}\xi}=0 \quad \text{at } \xi=0, \tag{11}$$

$$\frac{\mathrm{d}^2w}{\mathrm{d}\xi^2}=\frac{\mathrm{d}^3w}{\mathrm{d}\xi^3}=0 \quad \text{at } \xi=1. \tag{12}$$

4. Differential transform method

The differential transform of a function f in one variable is defined as follows

$$F[k]=\frac{1}{k!}\left(\frac{\mathrm{d}^kf(x)}{\mathrm{d}x^k}\right)_{x=x_0}. \tag{13}$$

And the inverse transformation is defined as

$$f(x)=\sum_{k=0}^{\infty}(x-x_0)^kF[k]. \tag{14}$$

Theorems that are frequently used in the transformation procedure are introduced in Table 1.

Table 1
Basic theorems of DTM

Original function	DTM
$f(x)=g(x)\pm h(x)$	$F[k]=G[k]\pm H[k]$
$f(x)=\lambda g(x)$	$F[k]=\lambda G[k]$
$f(x)=g(x)h(x)$	$F[k]=\sum_{l=0}^{k}G[k-l]H[l]$
$f(x)=\frac{\mathrm{d}^ng}{\mathrm{d}x^n}(x)$	$F[k]=\frac{(k+n)!}{k!}G[k+n]$
$f(x)=x^n$	$F[k]=\delta(k-n)=\begin{cases}0 & \text{if } k\neq n,\\ 0 & \text{if } k=n\end{cases}$

5. Solution

By applying the DTM to Eqs. (10)–(12) at $x_0 = 0$, and using the relationships defined in Table 1, the following equations are obtained:

$$W[0] = W[1] = 0, \tag{15}$$

and

$$\sum_{k=2}^{\infty} k(k-1)W[k] = \sum_{k=3}^{\infty} k(k-1)(k-2)W[k] = 0, \tag{16}$$

and

$$\begin{aligned}
&(k+1)(k+2)(k+3)(k+4)W[k+4] - (6c+3ck)(k+1)(k+2)(k+3)W[k+3] \\
&+ \left[6c^2 + 12c^2k + 3c^2\left(k^2-k\right) - \frac{\gamma^2}{6}(3+6\delta-3\delta c-2c)\right](k+1)(k+2)W[k+2] \\
&- \left[6c^3k + 6c^3\left(k^2-k\right) + c^3(k-2)\left(k^2-k\right) - \gamma^2\delta(k+1)\right](k+1)W[k+1] \\
&+ \left[-\omega^2 + \gamma^2(k-\delta ck) + \frac{\gamma^2}{2}\left(k^2-k\right)(1-\delta c)\right]W[k] \\
&+ \left[\omega^2 c - \gamma^2(ck-c) - \frac{\gamma^2 c}{3}(k-2)(k-1)\right]W[k-1] = 0.
\end{aligned} \tag{17}$$

Here $W[k]$ is the differential transform of $w(\xi)$. By using Eqs. (15–17), $W[k]$ values for $k = 4, 5, 6, 7\ldots$ can now be evaluated in terms δ, ω, c_2, c_3 and γ. These values were achieved by using the Mathematica software package. The results for the values $c = 0$, $\delta = 0$ and $n = 1$ are as follows

$$W[2] = c_2,$$

$$W[3] = c_3,$$

$$W[4] = \frac{c_2k^2}{24},$$

$$W[5] = \frac{c_3k^2}{40},$$

$$W[6] = \frac{c_2k^4}{1440} - \frac{c_2k^2(3-\omega^2)}{360},$$

$$W[7] = \frac{c_3k^4}{3360} - \frac{c_3k^2(6-\omega^2)}{840},$$

$$W[8] = -\frac{c_2k^4(10-\omega^2)}{40320} + \frac{k^2}{112}\left[\frac{c_2k^4}{1440} - \frac{c_2k^2(3-\omega^2)}{360}\right].$$

The coefficients are obtained to numerical accuracy and the constants c_2 and c_3 that appear in $W[k]$'s are given by

$$c_2 = W[2] = \frac{1}{2!}\left(\frac{d^2w}{d\xi^2}\right)_{x=0}, \quad c_3 = W[3] = \frac{1}{3!}\left(\frac{d^3w}{d\xi^3}\right)_{x=0}. \tag{18}$$

6. Results and discussion

For various values of the nondimensional hub radius, δ, and the nondimensional angular velocity, γ, and for the value $n = 1$, the nondimensional natural frequencies, ω are to be determined. In Table 2, variation of the first three nondimensional natural frequencies with respect to nondimensional angular velocity, γ, is shown together with comparative values reported in literature [6,7]. The taper ratio, c, is taken to be 0.5 in the analysis. The angular velocity and hub radius have significant effects on the values of the natural frequencies as can be seen from the results shown in Table 2. For a better insight and also in order to establish the trend, these effects are shown in Fig. 2. The lowest three nondimensional natural frequencies are plotted for two cases of the nondimensional hub radius, δ. The nondimensional natural frequencies, ω, increase as the nondimensional angular velocity, γ, increases and the rate of increase becomes larger with the increase in δ. This is due to the effect of centrifugal tension force which increases as the angular velocity and the hub radius are increased, as expected [8]. In Table 3, variation of the natural frequencies with respect to the taper ratio, c, is given and in Fig. 3, these calculated values are plotted.

Table 2
Variation of the first three nondimensional natural frequencies, ω, with respect to the nondimensional angular velocity, γ, and the nondimensional hub radius, δ, for $c = 0.5$ and $n = 1$

Nondimensional angular velocity, γ	Nondimensional natural frequency, ω	$\delta = 0$		$\delta = 2$	
		DTM	Ref. [6]	DTM	Ref. [7]
1	ω_1	3.98662	3.98660	4.38668	4.38580
	ω_2	18.47400	18.47400	18.87950	18.87400
	ω_3	47.41700	47.41700	47.83080	47.81500
2	ω_1	4.43680	4.43680	5.74260	5.74170
	ω_2	18.93660	18.93700	20.47300	20.46800
	ω_3	47.87160	47.87200	49.48660	49.47200
3	ω_1	5.09268	5.09270	7.45275	7.45190
	ω_2	19.68390	19.68400	19.87947	22.87400
	ω_3	48.61890	48.61900	52.12050	52.10600
4	ω_1	5.87796	5.87880	9.31032	9.30940
	ω_2	20.68500	20.68500	25.86624	25.86100
	ω_3	49.64560	49.64600	55.58160	55.56700

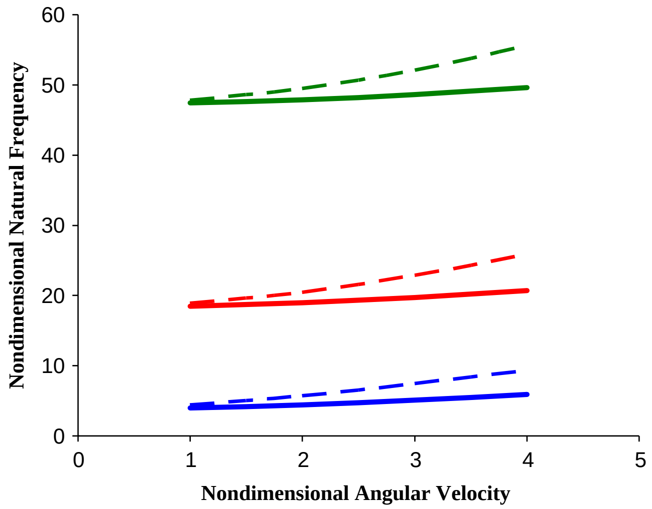

Fig. 2. Variation of the nondimensional natural frequencies, ω, with respect to the nondimensional angular velocity, γ, and the nondimensional hub radius, δ. (——, $\delta = 0$; - - - -, $\delta = 2$) (Table 2).

Table 3
Variation of the nondimensional natural frequencies, ω, with respect to the taper ratio, c, for $n = 1$, $\delta = 0$ and $\gamma = 1$

Taper ratio, c	Nondimensional natural frequencies					
	ω_1	ω_2	ω_3	ω_4	ω_5	ω_6
0	3.68165	22.18101	61.84176	121.05092	200.01155	299.14398
0.1	3.72398	21.48633	59.12560	115.33684	190.29792	283.98056
0.2	3.77313	20.77109	56.33928	109.46858	180.31562	268.86012
0.3	3.83109	20.03269	53.47071	103.41803	170.01455	253.25597
0.4	3.90076	19.26810	50.50395	97.14744	159.32681	237.04102
0.5	3.98662	18.47401	47.41728	90.60393	148.15651	220.08215
0.6	4.09594	17.64739	44.17999	83.70989	136.36346	202.16917
0.7	4.24170	16.78843	40.74909	76.35410	123.75992	183.46700
0.8	4.45396	15.93941	37.14266	68.51031	110.26864	162.53781
0.9	4.84443	15.54665	34.26288	61.47543	97.15930	141.04833

As it can be seen from the results, the nondimensional natural frequencies increase as the angular velocity increases due to the stiffening effect of rotation, while they decrease as the taper ratio increases due to the softening effect resulting from the decrease of the cross-sectional area. However, it has been observed that a critical taper ratio exists, after which the frequencies of a rotating tapered beam reverse their trend of change. It is obvious that the stiffening effect due to rotation becomes more dominant than the softening effect resulting from the decrease of the cross-sectional area, thus rendering the beam stiffer [9].

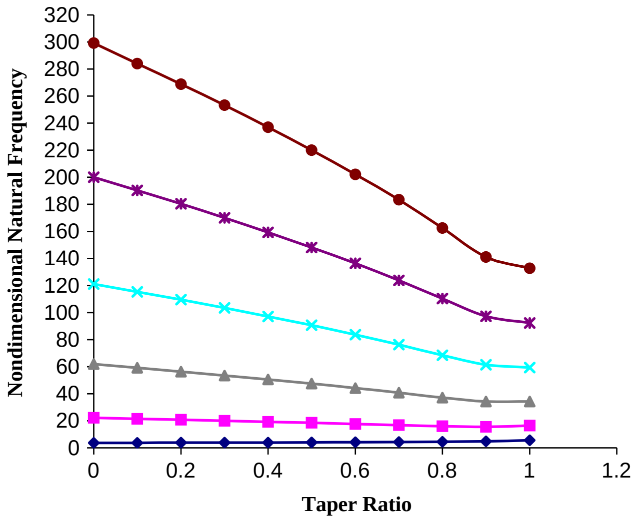

Fig. 3. Variation of the nondimensional natural frequencies with respect to the taper ratio, c, for the six lowest modes of the beam (Table 3).

References

[1] J.K. Zhou, *Differential Transformation and its Application for Electrical Circuits*, Wuhan, Huazhong University Press, Wuhan, China, 1986.

[2] Zeng, C.W. Bert, Vibration analysis of a tapered bar by differential transformation, *Journal of Sound and Vibration* 242 (2001) 737–739.

[3] J. Chung, H.H. Yoo, Dynamic analysis of a rotating cantilever beam by using the finite element method, *Journal of Sound and Vibration* 249 (2002) 147–164.

[4] J.R. Banerjee, A.J. Sobey, Energy expression for rotating tapered timoshenko beams, *Journal of Sound and Vibration* 254 (4) (2002) 818–822.

[5] D. Zhou, Y.K. Cheung, The free vibration of a type of tapered beam, *Computer Methods in Applied Mechanical Engineering* 188 (2000) 203–216.

[6] D.H. Hodges, M.J. Rutkowski, Free vibration analysis of rotating beams by a variable order finite element method, *American Institute of Aeronautics and Astronautics Journal* 19 (1981) 1459–1466.

[7] J.R. Banerjee, Free vibration of centrifugally stiffened uniform and tapered beams using the dynamic stiffness method, *Journal of Sound and Vibration* 233 (5) (2000) 857–875.

[8] H.H. Yoo, S.H. Shin, Vibration analysis of rotating cantilever beams, *Journal of Sound and Vibration* 212 (5) (1998) 807–828.

[9] A. Bazoune, Y.A. Khulief, A finite beam element for vibration analysis of rotating tapered Timoshenko beams, *Journal of Sound and Vibration* 156 (1) (1992) 141–164.